Geothermal solute equilibria. Derivation of Na-K-Mg-Ca geoindicators

WERNER F. GIGGENBACH

Chemistry Division, DSIR, Petone, New Zealand

Abstract—Relative Na, K, Mg, and Ca contents of thermal waters in full equilibrium with a thermodynamically stable mineral system derived through isochemical recrystallisation of an average crustal rock are, at a given temperature and salinity, uniquely fixed. Together with the compositions of waters resulting from isochemical rock dissolution, they provide valuable references for the assessment of the degree of attainment of fluid-rock equilibrium. In geothermal systems, the pair K-Na reaches its equilibrium contents as governed by

$$L_{kn} = \log\ (c_K/c_{Na}) = 1.75 - (1390/T)$$

most slowly (c_i in mg/kg, T in K). The quotient c_K^2/c_{Mg} adjusts much faster and to low temperatures ($<100°C$) according to

$$L_{km} = \log\ (c_K^2/c_{Mg}) = 14.0 - (4410/T).$$

The system K-Ca is sensitive to variations in f_{CO_2} with

$$L_{kc} = \log\ (c_K^2/c_{Ca}) = \log f_{CO_2} + 3.0.$$

These subsystems are combined to obtain graphical techniques for the evaluation of deep temperatures and CO_2-partial pressures by use of Na, K, Mg and Ca contents of geothermal water discharges.

INTRODUCTION

IN DYNAMIC HYDROTHERMAL alteration systems overall fluid-rock equilibrium is rarely attained and the fluids sampled are likely to have reached some complex steady-state composition reflecting the combined effects of initial fluid composition, the kinetics of primary mineral dissolution and secondary mineral deposition at changing temperatures and pressures, in addition to vapor loss, dilution and mixing with fluids of different origin. In the midst of all these complexities two limiting processes controlling the chemistry of thermal fluids may be distinguished: The first of these more or less hypothetical processes corresponds to isochemical dissolution of the rock material in contact with the rising fluid; the other to eventual equilibration of the fluid with the thermodynamically stable alteration assemblage resulting from isochemical recrystallisation of the primary rock at a given temperature and pressure, a process likely to come to completion only in stagnant systems of infinite age (GIGGENBACH, 1984). The chemical composition of fluids and minerals resulting from both these reference processes, however, are accessible to rigorous evaluation.

By exploiting differences in the thermodynamic properties and relative abundances of the four major cations encountered in crustal rocks and geothermal waters, Na, K, Mg and Ca, an attempt is made to derive geoindicators allowing water-rock equilibration conditions and the position of a given water sample with respect to the above two limiting states to be evaluated.

POTENTIAL PROCESSES AFFECTING THE CHEMICAL COMPOSITION OF THERMAL WATERS DURING THEIR MOVEMENT THROUGH THE CRUST

In an earlier investigation into mass transfer processes in hydrothermal systems involving the rise of initially magmatic fluids through intermediate to acid crustal rocks (GIGGENBACH, 1984), four major alteration processes and associated environments were identified:

1. Potassium metasomatism accompanied by silicification in major upflow zones.

2. Hydrogen metasomatism caused by the attack of CO_2 on Ca-aluminium silicates leading to the formation of calcite and Al-enriched, argillic to phyllic alteration assemblages principally over parts of the hydrothermal system subject to rapid conductive cooling or dilution adjacent to major upflow zones.

3. Sodium, magnesium, calcium metasomatism associated with descending and heating solutions and, therefore, affecting rock over the meteoric recharge zones at the periphery of a hydrothermal system.

4. Isochemical recrystallisation and hydration over close to stagnant parts of a hydrothermal system.

In conjunction with findings on active volcanoes (GIGGENBACH, 1975a, 1987), a fifth alteration process, likely to prevail over the deep magmatic to hydrothermal transition zones of a hydrothermal system with close volcanic-magmatic associations, may be defined. It consists of the attack of strong acids (HCl, H_2SO_4, HF) formed through absorption of magmatic gases into deeply circulating groundwater and leads to wholesale rock destruction, advanced argillic alteration and silicification.

The alteration patterns thus delineated may be used to construct a revised and more detailed version of an earlier schematic diagram (GIGGENBACH, 1981) depicting the theoretical distribution of alteration zones in a hydrothermal system as shown in Fig. 1. Again the top of the degassing magma is placed at an arbitrary but reasonable depth of 8 km, isotherms were drawn by assuming uniform and isotropic permeability conditions and a geothermal gradient of 50°/km
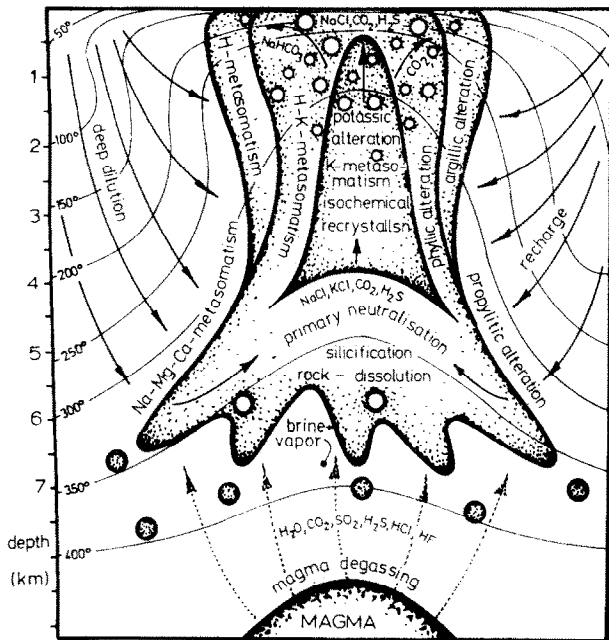
FIG. 1. Schematic cross-section of a hydrothermal system with close volcanic-magmatic associations.

HENLEY and McNABB (1978), BRIMHALL and GHIORSO (1983) and EUGSTER (1985). Fossil manifestations of such highly acid alteration environments are characterised by silicification and advanced argillic alteration (SILLITOE, 1973) or even complete cation leaching as at the volcanic hosted precious metal deposits at Summitville, Colorado (STOFFRE-GEN, 1985) or Temora, New South Wales (THOMPSON et al., 1986). The physical processes likely to accompany gas release from a solidifying magma body have been discussed by CATHLES (1977) and BURNHAM (1979).

With regard to the chemistry of the rising fluids, the major effects of their passing through the zone of primary neutralisation may be assumed to consist of the addition of Na, K, Mg and Ca in proportions close to those of the original rock and the conversion of much of the magmatic sulfur, initially in the form of SO_2 and H_2S, to pyrite at deep (GIGGENBACH, 1977; BRIMHALL, 1983), or alunite and anhydrite at shallower levels (GIGGENBACH, 1975b; KRUPP and SEWARD, 1987).

The fluids emerging from the zone of primary neutralisation are assumed to resemble closely those produced from deep wells in active geothermal systems. These close to neutral NaCl-KCl-brines still contain much of the originally magmatic CO_2 and some of the magmatic sulfur in the form of H_2S. Their very low magnesium and calcium contents point to early redeposition, possibly, still within the primary neutralisation zones, in the form of Mg- and Ca-rich alteration products such as amphiboles, biotite, chlorite, anhydrite and fluorite.

The major processes affecting the geothermal fluids proper during their further rise to the surface are minor hydrogen metasomatism, due to secondary neutralisation of CO_2, and potassium metasomatism. The very slow drop in temperature over the deeper central parts of the major fluid upflow zones is also conducive to isochemical internal re-equilibration of the rock components and therefore to the attainment of full fluid-rock equilibrium (GIGGENBACH, 1984).

On approaching the surface or the margins of the major upflow zones, temperature gradients become much steeper leading to a rapid increase in the reactivity of CO_2 with respect to hydrogen metasomatism. Separation of an increasingly CO_2 rich vapor phase and its absorption in shallow groundwater also generates an environment of increased acid alteration and the production of waters high in bicarbonate; depending on the duration of water-rock interaction, the relative proportions of cations acquired by the waters in these marginal zones may again approach those of the unaltered rock. Superficial oxidation of H_2S, especially in steam heated pools, provides another source of acidity and an environment for intense rock leaching (SCHOEN et al., 1974). The waters thus produced are low in chloride, but high in sulfate (ELLIS and MAHON, 1977).

Because of the dynamic nature of most hydrothermal alteration systems, the compositions of the waters present at any stage then are likely to reflect the transition between two limiting end member processes: from close to isochemical dissolution of crustal rock in highly aggressive, acid fluids, to equilibration with the thermodynamically stable mineral assemblage resulting from isochemical recrystallisation of such rock. In contrast to the intermediate waters, the compositions of the waters produced by these endmember pro-

outside the thermal system. There, and within the upflow zones, fluid pressures were assumed to correspond to the hydrostatic pressure of cold water, the temperature/depth distribution is that of CO_2-water mixtures in "full equilibrium" with K-mica, K-feldspar, chalcedony, calcite and the thermodynamically stable Ca-aluminium silicate (GIGGENBACH, 1984). The model of a hydrothermal alteration system thus obtained corresponds closely to that derived by LOWELL and GUILBERT (1970) on the basis of the lateral and vertical zoning of alteration in a wide range of prophyry ore deposits. Within the present context, it is used to delineate the processes likely to affect the chemical composition of hydrothermal fluids during their rise to the surface.

The composition of the fluids produced from the magma body at depth is not accessible to direct measurements. On the basis of the compositions of high temperature gases released from basaltic (GIGGENBACH and LE GUERN, 1976) and andesitic magmas (GIGGENBACH, 1987), they are likely to consist largely of water vapor containing between 20–40% b.w. CO_2, 5–10% b.w. total sulfur, predominantly in the form of SO_2 at low pressures, but H_2S at higher pressures, and 1 to 2% b.w. of HCl (ROSE et al., 1986). These fluids remain initially close to equilibrium with the rock. Because of the rapid increase in the dissociation constants of H_2SO_4 and HCl (RUAYA and SEWARD, 1987) with decreasing temperature, absorption of these gases into deeply circulating groundwater and cooling leads to the formation of acid, highly reactive solutions capable of virtually complete cation leaching of the wall rock and the production of waters with chloride and sulfate as the major anions. The mineralogical consequences of this "primary neutralisation" process were first evaluated by HEMLEY and JONES (1964), the likely involvement of magmatic fluids containing free HCl in the transport of ore metals was stressed among others by HOLLAND (1972),

cesses are accessible to rigorous evaluation. By comparing the chemical compositions of geothermal discharges with these theoretical compositions, the relative importance of rock dissolution and equilibration in controlling the chemistry of thermal waters may be assessed.

In earlier investigations into hydrothermal systems the re-distribution of ions between water and rock was frequently ascribed to an "ion exchange" process. Use of this term, however, should be reserved to the reversible exchange of ions in solution without destruction or change of the structure of the substrate. In hydrothermal systems, this type of ion exchange is restricted to the interaction of waters with a limited range of suitable clay minerals. The by far predominant processes facilitating the re-distribution of cations among solutions and minerals are rock dissolution (CHOU and WOLLAST, 1984; HOL-DREN and SPEYER, 1985) followed by solute transport and spatially independent deposition of secondary phases (GOGUEL, 1983; SAVAGE et al., 1987; SCHRAMKE et al., 1987; PETIT et al., 1987). Also, the term isochemical is preferred for processes involving the entire rock phase, the term congruent is reserved for the dissolution and recrystallisation of individual minerals.

Attainment of water-rock equilibrium depends to some degree on the kinetics of individual mineral dissolution and deposition reactions, but may to a first approximation be discussed in terms of the overall, steady-state rate of advancement of an alteration front with the amounts of rock components released during the dissolution stage being proportional to those present in the original rock. The composition of full equilibrium waters is likely to vary also with the chemical and mineralogical composition of the original rock (BORISOV et al., 1985). For the present purpose, the composition of waters in full equilibrium with intermediate to acid rocks is assumed to be determined only by temperature and salinity (ANORSSON et al., 1983a; GIGGENBACH, 1984).

CHEMICAL COMPOSITION OF THERMAL WATERS

In order to simplify correlation of water compositions and likely water-rock interaction environments, three well-characterised groups of waters were selected:

1. Highly acid chloride-sulfate waters likely to result from the absorption of magmatic gases in groundwater followed by close to isochemical dissolution of rock contacted. They are assumed to reflect conditions within the deep, primary neutralisation zone.

2. Spring waters associated with copious discharges of CO_2 (soda springs) and likely to be representative of the waters with high CO_2 reactivities at the periphery of hydrothermal systems.

3. Discharges from deep geothermal wells and from associated neutral chloride springs. These waters are likely to represent well-equilibrated fluids from the major upflow zones.

The first three samples of the first group of Table 1 are obviously volcanic waters, the White Island sample (WI) representing an emerald green water discharged from springs on the crater floor (GIGGENBACH and GLASBY, 1977), that from Ruapehu Crater Lake (RU), a water produced during an eruptive period (GIGGENBACH, 1975b). The next three samples are likely to be volcanic waters generated at depth but considerably diluted during their rise to the surface.

The second group comprises comparatively low temperature springs discharging copious amounts of free CO_2 (Soda Springs). The high chloride waters of the third group represent a wide range of deep geothermal well discharges and associated neutral chloride springs.

Temperatures for well discharges are those measured at depth, for spring discharges actually measured surface temperatures are given.

Of the seven soda waters, only two, Radkersburg (RA) and Te Aroha (TE) are actively depositing calcite at the surface. This observation is in agreement with values of +0.8 for the saturation index log (Q/K) based on the quotient $(a_{Ca^{2+}} \cdot a_{HCO_3^-}/a_{H^+})$. The pHs reported for all samples in Table 1 are those measured in the laboratory and, therefore, may differ considerably from those at depth. The saturation indices calculated by use of these pHs, therefore, are only valid at room temperature for the sample as analysed. Because of the comparatively shallow temperature dependence of the above equilibrium quotient, the values obtained may still reflect the original state of calcite saturation of the waters. It is for all other soda and chloride spring samples with ±0.4 close to equilibrium with calcite, except for Lake Nyos (LN) which was found to be well undersaturated with respect to this mineral (GIGGENBACH, 1988).

In Fig. 2, the waters are classified in terms of relative Cl^-, SO_4^{--} and HCO_3^- contents. The set of samples covers the entire spectrum of naturally occurring waters from virtually pure chloride waters, over mixed chloride-sulfate waters to bicarbonate waters largely produced from the soda springs.

A presentation in terms of the major cations is shown in Fig. 3. By comparison with the compositions of waters produced through isochemical dissolution of crustal rocks, such as basalt (BA), granite (GR) and the average crust (AC) (TAYLOR, 1964) and the composition of waters expected for equilibrium with an isochemically recrystallised, thermodynamically stable average crustal rock (GIGGENBACH, 1984), only the deep well discharges appear to achieve full water-rock equilibrium. The acid waters and the soda springs occupy positions suggesting varying degrees of approach to full equilibrium at lower temperatures. Most neutral chloride waters appear to follow a common curved trend suggesting the transition from rock dissolution to rock equilibration to be a process more complex than simple end member mixing. A more detailed evaluation of these rock-dissolution, rock-equilibration processes requires the set of four cations to be subdivided into several sub-sets such as Na-K, K-Mg, K-Ca.

COMPARISON OF ANALYTICAL AND THEORETICAL ACTIVITY QUOTIENTS INVOLVING Na-K-Mg

The first ionic solute geothermometer is based on early observations of a general decrease in Na/K ratios of thermal waters with increasing temperature (WHITE, 1957; ELLIS and WILSON, 1960; ELLIS and MAHON, 1964). Initial calibration of this Na-K geothermometer (WHITE, 1965; ELLIS and MAHON, 1967) led to relationships with quite shallow temperature dependences (Fig. 4), largely due to the inclusion of incompletely equilibrated spring waters. By taking into consideration experimental data on cation exchange between coexisting alkali feldspars (ORVILLE, 1963; HEMLEY, 1967), FOURNIER and TRUESDELL (1973) arrived at a revised calibration curve with a considerably steeper temperature dependence. Two further curves proposed later on the basis of findings by White and Ellis (TRUESDELL, 1975) and on geothermal well discharges in Iceland (ARNORSSON et al., 1983b) led to only minor modifications (1983A, Fig. 4).

In 1979, Fournier provided a revised equation, now based on Na and K contents of waters with well established thermal histories, such as deep geothermal well discharges and oil field brines. The resulting correlation (1979) approaches very closely that calculated by use of recent thermodynamic data on the stability of Na- and K-feldspars (BOWERS et al., 1984).

TABLE 1

Chemical composition of thermal water discharges, seawater and solutions of
100g of crustal rocks in 1kg of chloride water in mg/kg.

	Symb.	t(°C)	pH	Na	K	Mg	Ca	Cl	SO₄	HCO₃	ref.
Acid Springs											
White Island, NZ	WI	98°	0.6	5910	635	3800	3150	38700	4870	--	a
Kawa Idjen, Indon.	KI	60°	0.6	1030	1020	680	770	21800	62400	-	a
Mt Ruapehu, NZ	RU	38°	1.2	1120	170	1750	1380	13240	14700	-	a
Tamagawa, Japan	TA	98°	1.3	38	30	35	95	2970	2300	-	a
Guayabal, C. Rica	MV	64°	1.9	56	2	48	99	684	2830	-	a
B.Georginas, Guatem.	ZU	74°	2.0	134	32	26	72	16	1520	-	a
Soda Springs											
Waitangi, NZ	WA	49°	7.3	285	24	9	17	364	49	202	a
Omapere, NZ	NG	30°	6.9	62	9	10	37	25	<1	295	a
Golden Spr., NZ	GS	45°	7.0	224	20	7	11	51	8	670	a
Lake Nyos, Cameroon	LN	23°	5.7	19	7	58	45	1	<1	724	a
Acque Albule, Italy	AA	22°	6.1	138	22	238	1042	163	1470	1403	a
Radkersburg, Austria	RA	72°	8.9	2215	182	47	3	264	398	4130	a
Te Aroha, NZ	TE	79°	8.1	2920	67	4	7	540	1260	6830	a
Geothermal Wells, Springs											
Ngawha NG-9, NZ	NG	230°	7.7	893	79	0.110	3	1260	18	185	a
Jubilee Pool, NZ	NG	56°	7.2	842	72	1.600	9	1180	174	393	a
Wairakei, WK-66, NZ	WK	240°	8.5	995	142	0.040	17	1675	30	<5	a
Champagne Pool, NZ	WK	99°	8.0	1070	102	0.400	26	1770	26	76	b
Broadlands BR-11, NZ	BR	260°	7.4	675	130	0.011	1	964	41	376	a
Ohaki Pool, NZ	BR	98°	7.1	860	82	0.100	3	1060	100	680	b
Miravalles 10.C. Rica	MV	250°	7.8	1750	216	0.100	59	2910	40	27	a
Sal. Bagaces, C. Rica	MV	74°	8.6	2063	85	6.600	33	2700	102	739	a
Zunil ZQ-3, Guatem.	ZU	295°	8.1	933	231	0.012	15	1810	31	51	a
Zunil Spring	ZU	95°	7.0	384	32	39	17	172	234	635	a
Cerro Prieto, Mexico	CP	280°	7.3	5600	1260	0.270	333	10500	14	40	b
Spring N29, Mexico	CP	80°	7.6	5120	664	4.600	357	8790	31	65	b
Tongonan, Philipp.	TO	330°	7.0	3580	1090	0.200	128	6780	16	12	b
Banati Spring, Phil.	TO	98°	8.3	1990	210	0.400	86	3400	74	7	b
Morere Spring, NZ	MO	47°	7.0	6690	84	79	2750	15670	<3	28	a
Salton Sea, Well, USA	SS	330°	5.2	38400	13400	10	22010	118400	4	140	b
Seawater	SW	4°	7.8	10760	390	1290	410	19340	2710	140	
Rock solutions											
basalt	BA	-	--	1900	800	4500	6700	28650	-	-	c
granite	GR	-	--	2800	3300	200	1900	11240	-	-	c
average crustal rock	AC	-	--	2400	2100	2300	4200	19740	-	--	c

refs. a - this work. b - Henley et al. (1984). c - Taylor (1964)

Another correlation (1983G), showing an even steeper temperature dependence was proposed by GIGGENBACH et al., in 1983. It also is based on analytical data for a wide range of deep well discharges including those reported by FOURNIER

FIG. 2. Relative Cl, SO₄ and HCO₃ contents (mg/kg) of waters listed in Table 1.

(1979) and FOURNIER and POTTER (1979). Assuming equilibrium Na/K-values to be approached from "below" (Fig. 4), the latter line was obtained by connecting data points representing maximum Na/K-ratios at a given temperature.

In addition to these empirical lines and the theoretical albite-K-feldspar boundary, three horizontal lines corresponding to the isochemical dissolution of an average basalt, an average granite and an average crustal rock of intermediate to acid composition (TAYLOR, 1964) are shown in Fig. 4. The triangular space thus delineated is assumed to cover the compositional range of waters affected to varying degrees by isochemical rock dissolution and partial or complete equilibration with a thermodynamically stable mineral assemblage including albite and K-feldspar. Data points were plotted by converting analytical concentrations c_i in mg/kg to activities a_i according to

$$a_i = c_i \dot{\gamma}_i / 1000 \, M_i \qquad (1)$$

where $\dot{\gamma}_i$ is the total or stoichiometric ion activity coefficient of the solute species i and M_i its atomic weight. The equilibrium constant governing the reaction
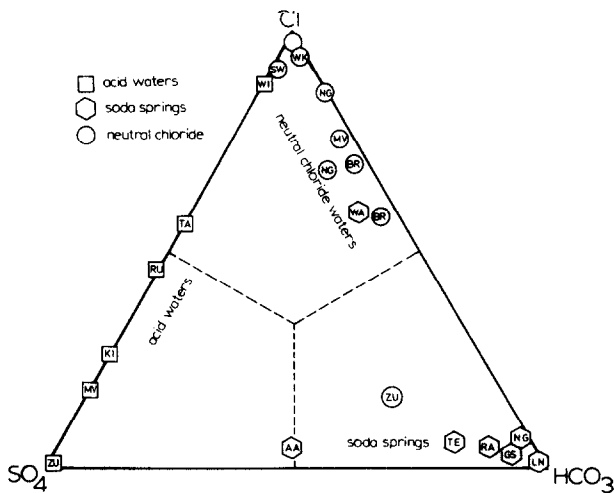
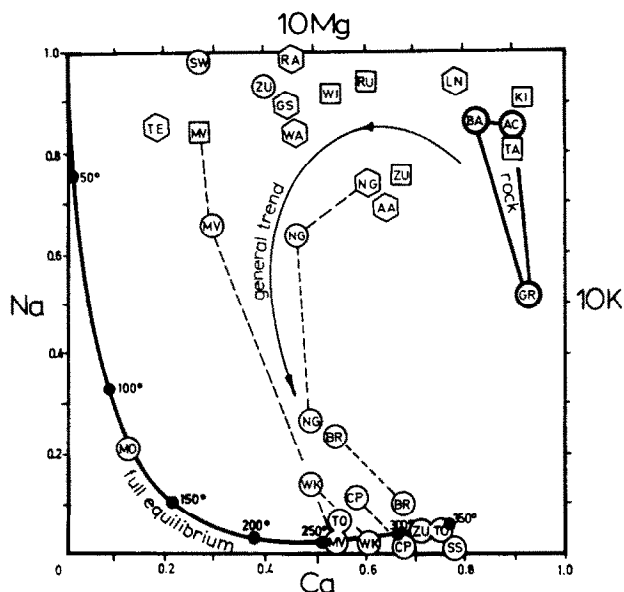$$\text{albite} + K^+ = \text{K-feldspar} + Na^+ \qquad (2)$$

FIG. 3. Plot of $10c_{Mg}/(10c_{Mg} + c_{Ca})$ versus $10c_K/(10c_K + c_{Na})$ of waters listed in Table 1 (c_i in mg/kg). The compositions of waters expected for attainment of full equilibrium with an average crustal rock as a function of temperature and of solutions of basalt (BA), granite (GR) and an average crustal rock (AC) are shown. For symbols see Table 1 and Fig. 2.

then becomes, with $\bar{\gamma}_{Na^+} = \bar{\gamma}_{K^+}$,

$$K_2 = (a_{Na^+}/a_{K^+})(a_{K\text{-feldspar}}/a_{albite})$$

$$\simeq 1.7\ c_{Na^+}/c_{K^+}. \tag{3}$$

The activity ratio $a_{K\text{-feldspar}}/a_{albite}$ for the secondary feldspars may safely be assumed to be close to unity.

Data points for deep geothermal well discharges fall close to the theoretical albite/K-feldspar coexistence line suggesting close attainment of fluid-rock equilibrium. Na/K ratios of associated spring discharges are generally shifted to higher values, pointing to some re-equilibration of the spring waters during their rise to the surface. Corresponding Na/K equilibration temperatures, however, are only some 50° below deep well temperatures suggesting Na/K ratios to be quenched at considerable depth. The sample MO represents a vigorous discharge of a 47° high chloride water, its inferred equilibration temperature is with 90°C also very low. Seawater (SW) plots well within the stability field of K-feldspar and is obviously far from equilibrium with albite.

Of the highly acid waters, two show Na/K-ratios corresponding to isochemical leaching of crustal rocks (KI, TA), the remainder have increased Na/K-ratios suggesting preferential leaching of sodium or removal of some of the potassium in the form of secondary alteration products. Under the acid conditions, K-containing aluminium silicates are unstable, the most likely K-mineral to form is alunite (HEMLEY and JONES, 1964). Actual deposition of this mineral has been reported for both the White Island (WI) and Ruapehu (RU) waters (GIGGENBACH, 1975b). No surface deposition of alunite has been reported for the two remaining acid waters as discharged at Guayabal, Costa Rica (MV) and Baños Georginas, Guatemala (ZU); their high Na/K-ratios may be ascribed to the deposition of K-Al-sulfates at depth.

Waters from soda springs occupy positions close to those of the acid waters. Their generally much lower acidity should allow aluminium silicates to form, their increased Na/K-ratios then may be ascribed to the removal of K in the form of K-rich clays. Of the CO_2 waters, that of Lake Nyos, Cameroon (LN), has a composition compatible with dissolution of local basalt (GIGGENBACH, 1988). Only the Te Aroha (TE) water, New Zealand, shows close approach to full equilibrium with the rock.

Of the waters considered here, the deep well discharges have Na and K contents compatible with attainment of water/feldspar equilibrium. The acid and CO_2-rich waters occupy positions intermediate between rock dissolution and equilibration. The apparent partial re-equilibration thus indicated may be due to preferential leaching of sodium or the removal of K-rich alteration products such as alunite at high, clays at lower acidities, but is unlikely to reflect attainment of equilibrium with feldspar at temperatures much higher than discharge temperatures. The acidity and high sulfate contents of the first group of waters provide early warning signs that Na/K-temperatures are likely to be unrealistic; in the case of the close to neutral, low sulfate, high CO_2 waters no such ready warning signals are apparent.

The strong dependence of Mg contents on the temperature of thermal discharges has long been recognised and has generally been ascribed to equilibration with chlorite (ELLIS, 1971) or Mg containing clays for which chlorite may serve as a thermodynamic proxy. By use of theoretical considerations, two potential mineral systems likely to control magnesium contents of geothermal discharges were identified, chlorite over parts of the hydrothermal system still affected by hydrogen metasomatism, biotite as a component of a fully equilibrated, isochemically recrystallised alteration assemblage (GIGGENBACH, 1984). Uncertainties in the activities of the clinochlore and phlogopite endmembers, arising from the large compositional variations of naturally occurring chlorites and biotites, the close similarity in the thermodynamic behaviour of the two mineral systems, and the ubiquitous presence of chlorite in hydrothermal alteration assemblages suggest that the behaviour of magnesium in waters
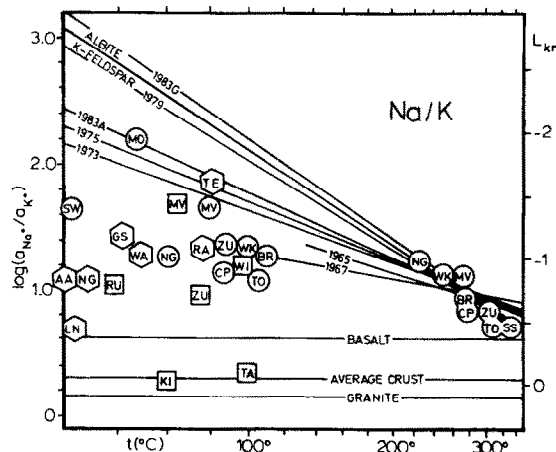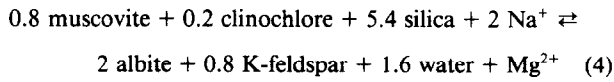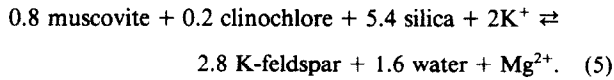

FIG. 4. Empirical, theoretical and analytical Na/K-activity ratios of thermal waters as a function of temperature. For symbols see Table 1 and Fig. 2.

approaching attainment of full equilibrium may adequately be described, in terms of endmember components, by the reactions

$$0.8 \text{ muscovite} + 0.2 \text{ clinochlore} + 5.4 \text{ silica} + 2\,Na^+ \rightleftharpoons$$

$$2 \text{ albite} + 0.8 \text{ K-feldspar} + 1.6 \text{ water} + Mg^{2+} \quad (4)$$

and

$$0.8 \text{ muscovite} + 0.2 \text{ clinochlore} + 5.4 \text{ silica} + 2K^+ \rightleftharpoons$$

$$2.8 \text{ K-feldspar} + 1.6 \text{ water} + Mg^{2+}. \quad (5)$$

The generally observed supersaturation of geothermal solutions with respect to silica is taken into account by assuming its activities to be controlled by equilibrium with its microcrystalline form, chalcedony; water fugacities are controlled by the presence of liquid water. Corresponding equilibrium constants then become

$$K_4 = (a_{Mg^{2+}}/a_{Na^+}^2)(a_{albite}^2 a_{K\text{-feldsp.}}^{0.8}/a_{musc.}^{0.8} a_{clinochlore}^{0.2}) \quad (6)$$

$$K_5 = (a_{Mg^{2+}}/a_{K^+}^2)(a_{K\text{-feldsp.}}^{2.8}/a_{musc.}^{0.8} a_{clinochlore}^{0.2}). \quad (7)$$

Values for K_4 and K_5 were obtained by use of the hydrolysis constants provided by BOWERS et al. (1984), their resulting temperature dependences are shown in Figs. 5a and 5b for activities of unity of the endmember phases involved.
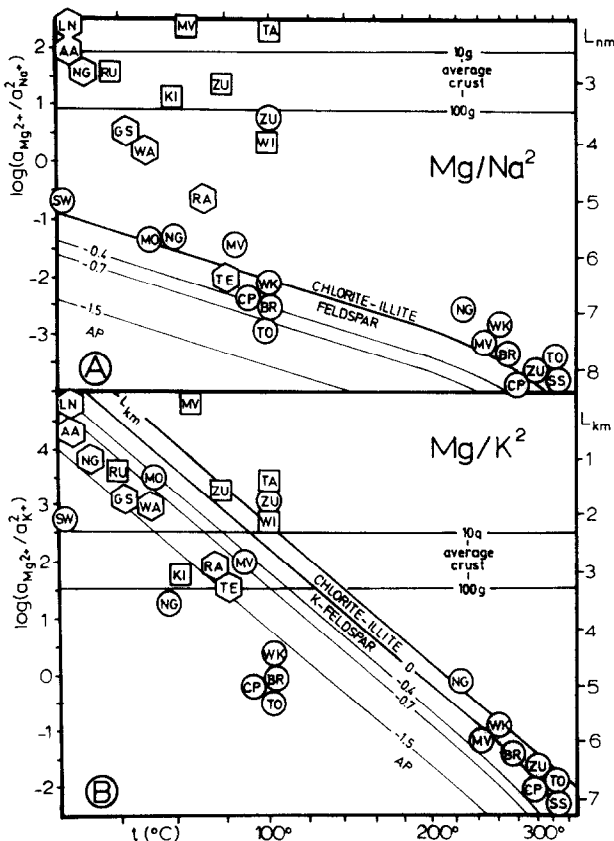

FIG. 5. Empirical, theoretical and analytical activity quotients involving Na (A), K (B) and Mg. Chlorite-illite-feldspar coexistence lines are shown as a function of variations in mineral activities according to Eqn. (8). For symbols see Table 1 and Fig. 2, AP = log $(a_{muscovite}^{0.8} a_{clinochlore}^{0.2})$.

The effect of the incorporation of muscovite and clinochlore into naturally occurring illites and chlorites may be assessed by use of their activities reported by CAPUANO and COLE (1982) for drill cuttings from the Roosevelt Hot Springs and by WALSHE (1986) for a wide range of hydrothermal layer silicates. For these samples, values of log $a_{muscovite}$ vary from -0.73 to -0.15 with a mean of -0.33, log $a_{clinochlore}$ from -4.7 to -1.3 with a mean of -2.2. The activities of the feldspar endmembers may safely be assumed to be close to unity, the logarithm of the activity product AP = log $(a_{muscovite}^{0.8} a_{clinochlore}^{0.2})$ then may vary from -1.5 to -0.4 with a mean of -0.7. The effect on log $(a_{Mg^{2+}}/a_{M^+}^2)$ corresponds to

$$\log (a_{Mg^{2+}}/a_{M^+}^2) = \log K_j + \log (a_{muscovite}^{0.8} a_{clinochlore}^{0.2}) \quad (8)$$

as shown in Fig. 5 for the above limits. The rock dissolution process is indicated by two lines representing the dissolution of 10 g and 100 g of an average crustal rock in 1 kg of water. Comparison of analytical and theoretical information again is based on Eqn (1). For the isocoulombic reactions considered here, the activity coefficients for mono- and di-valent ions can be assumed to be closely related through $\dot\gamma_1^2 = \dot\gamma_2$ (LINDSAY, 1980).

In the case of $a_{Mg^{2+}}/a_{Na^+}^2$ (Fig. 5a), deep well discharges plot close to the theoretical lines albeit with a tendency to deviate to higher relative Mg contents. Associated spring discharges are shifted parallel to the theoretical trend apparently suggesting maintenance of water-rock equilibrium during their rise to the surface. An exemption are the samples from the Zunil area in Guatemala (ZU) where the neutral spring discharge appears to be strongly affected by admixture of the nearby high sulfate water (B. Georginas).

All acid waters occupy positions far from the equilibrium lines and over a range expected for rock dissolution. Of the soda springs, Te Aroha (TE) and Radkersburg (RA) appear to approach equilibrium most closely. The compositions of Lake Nyos (LN), Acque Albule (AA) and Omapere Soda Spring (NG) are likely to be controlled by rock dissolution rather than equilibration. At a temperature of $4°C$, the composition of seawater would be compatible with full equilibrium with respect to reaction (4).

The distribution of data points in Fig. 5a clearly shows that relative Na/Mg-contents of acid waters and of most of the soda springs are close to those expected for dissolution of crustal rock suggesting that preferential leaching of Na, to give rise to the high Na/K-values of Fig. 4, is not important. The increased Na/K-ratios, therefore, are more likely to be due to the deposition of K-rich alteration phases.

The K, Mg-contents of deep well discharges again point to close attainment of equilibrium with respect to Eqn. (5) (Fig. 5b). Associated springs are shifted to higher a_{Mg}/a_K^2-values, again quench temperatures some $50°$ below their deep temperatures are indicated. Instead of being significantly removed from the rock equilibration lines as in Fig. 4, the compositional ranges of dissolved rock now coincide with equilibrium compositions over low to intermediate temperatures. The position of data points for the acid waters close to the rock equilibrium line, therefore, is not too surprising; the position of some well above the rock dissolution range (MV, TA) again points to the deposition of K-rich minerals.

In contrast to Fig. 5a, the compositions of soda springs agree with attainment of equilibrium with respect to reaction (5), suggesting that the system K-Mg approaches mineral-fluid equilibrium at temperatures down to $25°$ even in a comparatively aggressive environment. The thermodynamic

behaviour of the K-Mg-clays, likely to form at these low temperatures, appears to be still described adequately by their thermodynamic proxies muscovite and clinochlore.

The obviously fast response to variations in temperature renders K, Mg contents highly suitable as the basis for a geothermometer. The temperatures obtained, however, will always be close to those measured anyway. On the other hand, the fast response of this system may provide the means to differentiate among the various processes interfering with the evaluation of deep equilibration temperatures by use of the system Na-K. The findings provided by Figs. 4 and 5 also show that both rock dissolution and equilibration play an important part in determining the chemical compositions of thermal waters. In order to assess the relative importance of these processes on the individual constituents Na, K, Mg, Ca, a more detailed discussion of the evolution of thermal waters during the transition from rock dissolution to equilibration is required.

VARIATIONS IN SOLUTE CONTENTS AS A FUNCTION OF ROCK DISSOLUTION AND EQUILIBRATION

In an earlier investigation into mass transfer processes in hydrothermal alteration systems, the reaction path of solutions resulting from the dissolution of and equilibration with an average crustal rock was described in terms of $Al_H = \log (a_{Al^{3+}}/a^3_{H^+})$ versus silica diagrams (GIGGENBACH, 1984). A simplified version for 200°C is given in Fig. 6. It was constructed by assuming dioctahedral alkali clay minerals to belong to a continuous solid solution series involving the endmembers muscovite and pyrophyllite as described earlier (GIGGENBACH, 1985). In case recent suggestions are valid that illite and smectite represent distinct phases (SASS et al., 1987), the smooth feldspar-clay boundary curves would be replaced by a series of chords marking feldspar-illite and feldspar-smectite coexistence, without changing the overall correlations in any significant way.

During the initial dissolution stages, both Al and silica in solution are assumed to increase in proportion to the amount of rock dissolved

FIG. 6. The stability of Na- and K-aluminium silicates as a function of the activity of dissolved silica and $Al_H = \log (a_{Al^{3+}}/a^3_{H^+})$ at 200°C. Arrows depict likely path of solutions during the transition from rock dissolution to rock-equilibration.

until kaolinite precipitates. From then onwards the system moves along the kaolinite boundary until the solution becomes saturated with respect to solid silica (chalcedony, quartz). At fixed silica activities, ongoing rock dissolution will shift Al_H-values to lower values (SAVAGE, 1986) until a state corresponding to equilibrium with a thermodynamically stable assemblage formed from the original rock is reached. For an average crustal rock the mineralogical composition of this assemblage contains Na in the form of albite, Mg either as chlorite or biotite, Ca as one of the aluminium silicates, represented by the their thermodynamic proxies laumontite at low temperatures and wairakite at high temperatures; K-feldspar and mica provide the buffer to accommodate any aluminium not incorporated into the above mineral phases. The final stage of the alteration process, therefore, is delineated by the intersection of the quartz solubility line with the K-mica-feldspar coexistence boundary (full equilibrium).

According to this reaction sequence, secondary albite may be expected to form well before K-feldspar. A look at Figs. 4 and 5, however, indicates that equilibrium with K-feldspar is obviously much more readily attained than with albite, most of the lower temperature waters plotting well outside the stability fields of Na-feldspar. The major reason for this discrepancy is the fact that two-dimensional projections of multicomponent systems such as Fig. 6 provide only an indication of the potential stability not necessarily the actual formation of a given mineral. For a mineral to form, the solution has to be saturated with respect to all the components involved in its deposition. The Al_H-silica-diagram of Fig. 6 takes into account only Al^{3+}, H^+ and SiO_2-activities; albite, however, is only able to form if the activities of the additional component Na^+ are also high enough.

During the initial interaction of an acid water with rock the amount of sodium added to the solution is assumed to be proportional to the amount of rock dissolved. The amount of sodium required for the stable formation of albite within the solute system Na-K-Mg-Ca-Cl may be calculated by use of the simple charge balance

$$m_{Na^+} + m_{K^+} + 2m_{Mg^{2+}} + 2m_{Ca^{2+}} = m_{Cl^-} \qquad (9)$$

and a procedure based on thermodynamic equilibrium constants for "ion exchange" reactions among the four cations in a fully equilibrated system as described earlier (GIGGENBACH, 1984). The distribution of solutes as shown in Fig. 7 was obtained accordingly by assuming attainment of full equilibrium between the solution and an assemblage containing albite, K-feldspar, muscovite, clinochlore and laumontite below, wairakite above 260°C. Relative concentrations of monovalent and divalent cations of Fig. 7 differ considerably from those shown earlier (GIGGENBACH, 1984) due to an arithmetical error in the calculation of the latter. Figure 7 here, therefore, replaces that of the earlier study. As already stated much earlier (HOLLAND, 1972; SHI-KAZONO, 1978), relative contents of divalent ions (Mg^{2+}, Ca^{2+}) increase at low salinities with the square of the chloride content. At all salinities, however, full equilibrium Mg and Ca contents decrease with temperature, potassium contents increase, with sodium at low salinities remaining independent of temperature but increasing with temperature considerably at high salinities. Cooling of fully equilibrated, highly saline solutions, therefore, may lead to both K- and Na-metasomatism; of dilute solutions (<1000 mg/kg Cl) only to K-metasomatism.

The full equilibrium cation contents thus derived may be compared to those released from the rock as shown in Fig. 8 for the reaction of a strong acid (HCl) with an average crustal rock. Initial rock dissolution is evaluated in terms of a titration according to

$$(M_{2/z}O) + 2H^+ \rightarrow 2/zM^{z+} + H_2O \qquad (10)$$

where M^{z+} is one of the metallic solution species Na^+, K^+, Mg^{2+}, Ca^{2+} present in the rock as the oxide component ($M_{2/z}O$). Release of silica does not consume protons, the rock component Al_2O_3 is also assumed to be quantitatively converted to hydroxy-minerals ($Al(OH)_3$, $AlOOH$) and "uncharged" aluminium silicates (kaolinite, pyrophyllite) without consuming protons. Initial rates of rock dissolution are likely
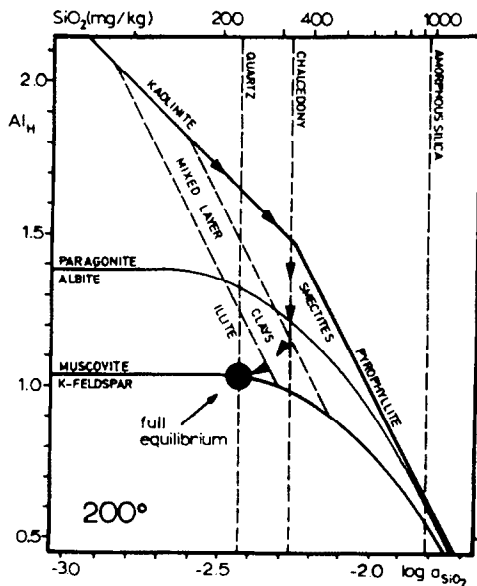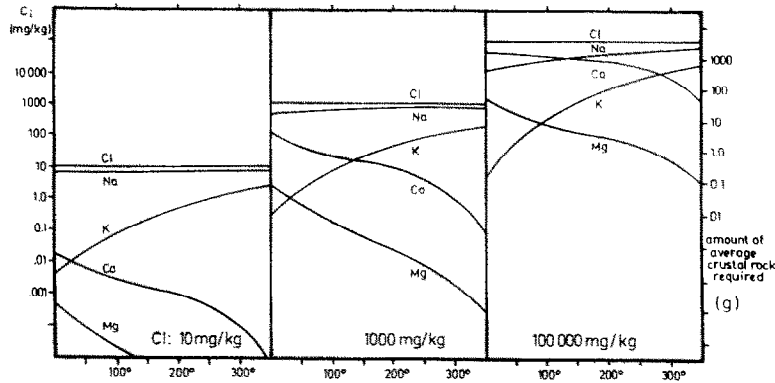
FIG. 7. Distribution of solute species (in mg/kg) in full equilibrium hydrothermal solutions as a function of temperature and chloride contents of 10, 1000 and 100,000 mg/kg (0.00028, 0.0283, 2.83 m).
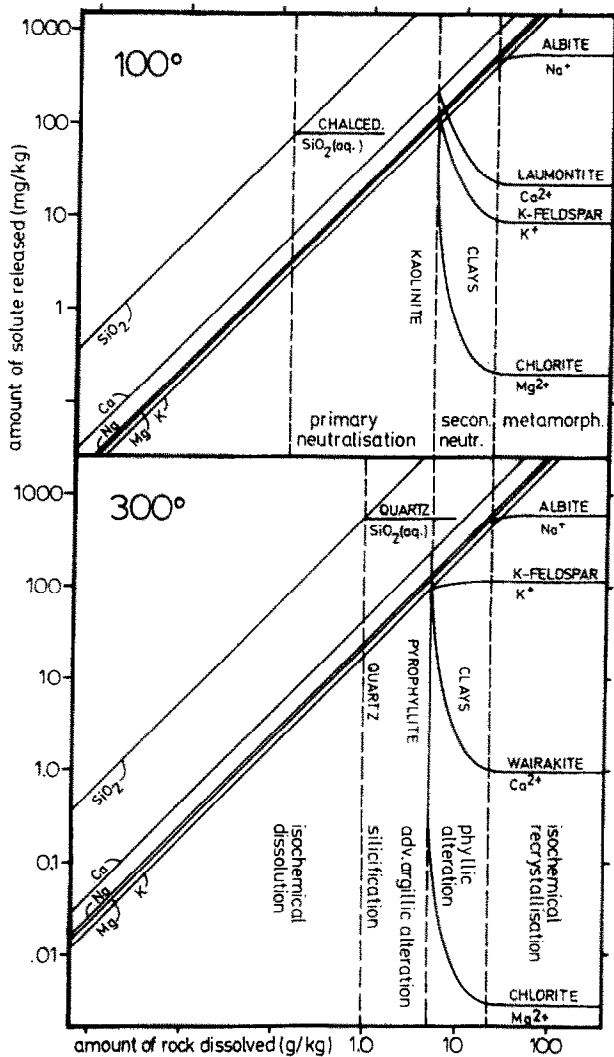

FIG. 8. Amounts of Na, K, Mg, Ca and SiO$_2$ released during the dissolution of increasing amounts of an average crustal rock in a 0.0283 m (1000 mg/kg Cl) solution of HCl at 100° and 300°C. On reaching saturation with respect to aluminium silicates, amounts of Na, K, Mg and Ca in solution decrease due to incorporation into respective alteration products.

to be fast, slowing down considerably as the "equivalence" point is reached. The drastic drop in proton activities on reaching this point will also lead to the immediate deposition of "charged" aluminium silicate such as smectites and chlorites. For the systems shown in Fig. 8, this point is reached after the dissolution of 5.1 g of an average crustal rock in 1 kg of an initially 0.028 m solution of HCl (1000 mg/kg of chloride).

The amounts of Mg and Ca released by then are well above those required for full equilibrium with chlorite and either laumontite (100°) or wairakite (300°), respectively. In accordance with Fig. 6, the minerals forming in this not-yet full equilibrium system, however, are likely to be various layer silicates typical of argillic to phyllic alteration assemblages. At both 100° and 300°, the amounts of sodium released at this stage are still well below those required to form a full equilibrium assemblage involving albite. Because of the essentially complete consumption of "free" protons further release of Na to the solution relies now on protons generated by the conversion of "acid" clays to more "neutral" aluminium silicates according to

$$z(\text{H-aluminium silicate}) + M^{z+} \rightarrow$$

$$(M\text{-aluminium silicate}) + z\text{H}^+. \quad (11)$$
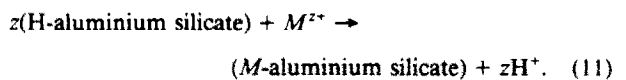
The comparatively low steady state proton activities maintained by this process can be expected to lead to very slow rates of rock dissolution and, therefore, to very slow rates of equilibration with respect to the system involving sodium. The amount of average crustal rock required to produce a 1000 mg/kg chloride solution in equilibrium with an assemblage containing albite is 15.4 g at 100°C and 14.5 g at 300°C (Fig. 7), three times that consumed in the fast primary neutralisation step. On attainment of full fluid-rock equilibrium, further rock alteration consists of very slow isochemical recrystallisation (metamorphism) of the remaining rock (Fig. 8).

During the "secondary neutralisation" process as symbolised by reaction (11), the relative concentrations of the three cations K$^+$, Mg^{2+}, and Ca^{2+}, can be expected to be initially controlled by the formation of "acid" clays in a thermodynamic environment still dictated by the composition of the fluid phase (fluid dominated) but

rapidly approaching the "rock dominated" environment of the full equilibrium assemblage (Fig. 8). In spite of non-attainment of full equilibrium, the solution still being undersaturated with respect to albite, the chemistry of K and Mg may quite early on be discussed in terms of partial equilibration within the system K-mica/K-feldspar and chlorite. The chemistry of Ca is complicated by the likely early formation of the non-aluminium silicate calcite in CO_2 containing systems, it, therefore, will be discussed separately. The presence of sulfate was also not considered in the construction of Fig. 8. It is likely to reduce both K and Ca contents through formation of alunite and anhydrite and, therefore, would affect the arrangement of alteration zones as given in Fig. 8 for simple chloride waters.

At temperatures above 200°, well discharges were found to be close to equilibrium with respect to both Na- and K-feldspar (Fig. 4). The preservation of these high temperature Na/K-ratios in associated surface spring discharges provides the basis for the most commonly used geothermometer. The coincidence of high temperature equilibrium Na/K-values with those for obviously unequilibrated acid waters, however, introduces large uncertainties in its application. In order to be able to judge the reliability of Na/K-temperatures an indicator is required allowing a distinction to be made among waters likely to have equilibrated with the rock or not.

The distribution of data points in Fig. 5a provides such a clear distinction between acid waters resulting from rock dissolution and waters approaching full rock equilibrium. The underlying large difference in the theoretical position of data points for rock dissolution and equilibration suggests that the system Na-Mg may form the basis for a parameter allowing equilibrated and unequilibrated waters to be separated. Use of this system as a geothermometer, by itself, is obviously impeded by the likely lack of equilibrium with respect to albite at low temperatures.

A solute system involving alteration phases forming early on in the rock equilibration process is that linking potassium and magnesium as shown in Fig. 5b. High temperature data points again fall close to the theoretical line representing co-existence of layer silicates with feldspar (Eqn. (7)) at end-member activities close to unity. Data points for lower temperature waters occupy positions corresponding to the likely attainment of equilibrium with naturally occurring K-Mg-layer silicates. The major distinction in the behaviour of the system K-Mg is the apparent attainment of solution-mineral equilibrium at very low temperatures and even for CO_2-rich waters as represented by the soda springs. The coincidence of the composition of some of the highly acid waters with that expected for equilibrium, however, is likely to be fortuitous and to result from the overlap of the compositional ranges for rock dissolution with those for rock equilibration at around 100°C and introduces considerable uncertainties in the application of the quotient Mg/K^2 as a geothermometer.

Summarising the three sub-systems considered above, the one involving Na-K is likely to respond most slowly and, therefore, to preserve deep equilibration Na/K-ratios. The production of similar ratios in waters obviously not in equilibrium with the rock generates large uncertainties in its application as a geothermometer. Use of the system Na-Mg as a geothermometer is limited by its shallow temperature dependence and its excessive sensitivity to the addition of non-equilibrated waters. Addition of even minor amounts of such waters leads to apparent temperatures of equilibration by far

too low. The system K-Mg appears to adjust most rapidly and to attain equilibrium values even for CO_2-rich waters. The overlap of rock dissolution values with equilibrium values again introduces uncertainties. Each of the above three sub-systems then has its peculiar advantages and disadvantages. By developing a technique allowing the simultaneous evaluation of the effects of rock dissolution and equilibration on the combined system Na-K-Mg, it may be possible to eliminate some of the drawbacks associated with separate evaluation.

SIMULTANEOUS EVALUATION OF WATER/ROCK EQUILIBRATION CONDITIONS FOR THE SYSTEM Na-K-Mg

Initial evaluation of correlations among three independent variables is most conveniently carried out by use of tri-linear or triangular diagrams. Their construction requires the conversion of absolute to relative values through application of a linear scaling or normalising factor. Because of the non-linear thermodynamic correlations among Na, K and Mg, comparison of analytical and theoretical information by use of standard triangular plots would only be valid for given values of $m_{Na^+} + m_{K^+} + 2m_{Mg^{2+}}$. In order to render the plot applicable at all salinities, relative Na, K, Mg-data have to be plotted in terms of either $m_{Na^+}^2$, $m_{K^+}^2$, $m_{Mg^{2+}}$ or m_{Na^+}, m_{K^+}, $\sqrt{m_{Mg^{2+}}}$, the latter conducive to a less "spread-out" presentation. In gaining the ability to represent data for solutions of any salinity in one diagram, one of the most valuable features of triangular plots, the presentation of mixing relationships by straight lines, had to be sacrificed. For processes consisting essentially of variations in relative Mg-contents, mixing lines still remain straight (Fig. 9).

Adoption of a triangular plot involving the variables m_{Na^+}, m_{K^+} and $\sqrt{m_{Mg^{2+}}}$ allows solution compositions representing attainment of full water-rock equilibrium for all salinities to be presented in terms of a single curve. In order to facilitate practical application, the concentration scale c_i in mg/kg (Eqn. (1)) is used, in order to accommodate most geothermal waters, sodium contents are divided by 1000, potassium by 100 and the square root is taken of magnesium values as measured. Because of their potential use as geothermometers, the activity quotients used in Figs. 4 and 5 are converted to concentration quotients with a positive temperature dependence. The temperature dependence of c_{K^+}/c_{Na^+} adopted here is that proposed earlier (GIGGENBACH et al., 1983) and shown in Fig. 4 (1983G) according to

$$L_{kn} = \log (c_{K^+}/c_{Na^+}) = 1.75 - (1390/T) \qquad (12)$$

where T is the absolute temperature in K. It is assumed to describe attainment of full water/feldspar equilibrium.

For the quotient $c_{K^+}^2/c_{Mg^{2+}}$ a temperature dependence parallel but 0.3 log-units above the theoretical line for the co-existence of K-feldspar with clinochlore and muscovite at endmember activities of unity is adopted (Fig. 5b). It is that, slightly rounded off, reported earlier (GIGGENBACH et al., 1983)

$$L_{km} = \log (c_{K^+}^2/c_{Mg^{2+}}) = 14.0 - (4410/T). \qquad (13)$$

Use of this temperature correlation is justified by the position of high temperature data points in Fig. 5b and the assumption
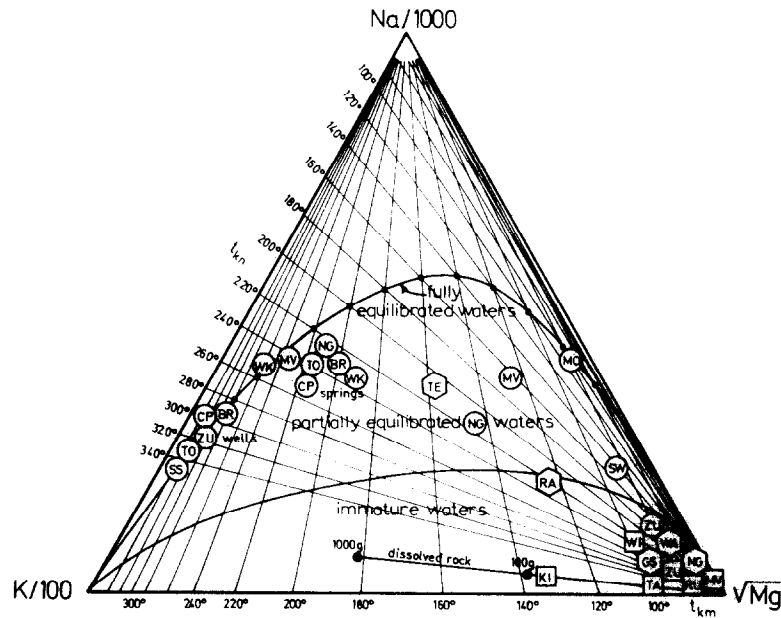
FIG. 9. Relative Na, K, Mg contents of thermal waters. Isotherms calculated by use of Eqns. (12) and (13) are given together with the full equilibrium curve. For symbols see Table 1 and Fig. 2.

that measured temperatures of the lower temperature waters are likely to be somewhat below actual water-rock equilibration temperatures. The deviation with regard to theoretical behaviour may also be ascribed to uncertainties in the thermodynamic data used for K-feldspar, muscovite and clinochlore. At present there appears to be no reason to favor a theoretical over the empirical trend.

The internally consistent temperature dependence of the quotient $c^2_{Na^+}/c_{Mg^{2+}}$ is simply obtained by use of

$$L_{nm} = L_{km} - 2L_{kn} = \log(c^2_{Na^+}/c_{Mg^{2+}})$$

$$= 10.5 - (1630/T). \quad (14)$$

In a fully equilibrated system each of the above three relationships is equally valid. As pointed out earlier, only the two sub-systems K-Na and K-Mg are likely to provide the basis for suitable geothermometers. They are presented in Fig. 9 by two sets of isotherms, their intersections correspond to the composition of waters in equilibrium with both mineral systems, the resulting curve is marked "full equilibrium". The compositions of waters formed through isochemical dissolution of an average crustal rock are shown in Fig. 9 for the dissolution of up to 1000 g in 1 kg of water. The rock dissolution line thus defined is well separated from the full equilibrium curve.

As expected, high temperature well discharges plot somewhat above actually measured deep temperatures on the full equilibrium line. Associated spring water compositions are shifted to lower temperatures and off the full equilibrium line indicating acquisition of Mg by the waters in response to decreasing temperatures to be faster than that of Na. The low temperature "formation water" discharge from Morere (MO) also plots on the full equilibrium line suggesting attainment of water-rock equilibrium, given enough time, even at quite low temperatures.

The position of data points for two soda spring discharges (TE, RA) points to attainment of partial equilibrium, the remaining soda spring waters and all the acid waters plot close to the Mg-corner. Data points in this area may then be taken to correspond to those of "immature" waters generally, to waters unsuitable for the evaluation of K/Na-equilibration temperatures. For not too acid waters, K/Mg-temperatures may still be valid. Of these acid waters, the composition of Kawa Idjen (KI) corresponds to the dissolution of 90 g of an average crustal rock, the others show reduced alkali contents indicating removal of some of the Na and K, possibly in the form of alunite, with Mg remaining unaffected by the deposition of secondary minerals. These conclusions are supported by observations on waters from Ruapehu Crater Lake during the 1971 active period (GIGGENBACH, 1975b).

Evaluation of analytical Na, K and Mg contents by use of Fig. 9 allows a clear distinction to be made between waters suitable or unsuitable for the application of ionic solute geothermometers. At the same time it allows deeper equilibration temperatures and the effects of a variety of processes such as re-equilibration and mixing of waters of different origins to be assessed for a large number of samples. The simultaneous evaluation facilitates also the delineation of trends and groupings among water discharges and, from these, of variations in the nature and intensity of processes affecting the rising waters.
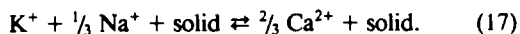
REACTIONS INVOLVING CALCIUM

The most popular ionic solute geothermometer presently in use is the Na-K-Ca-geothermometer as devised by FOURNIER and TRUESDELL (1973). By assuming the three cations to be linked through the general reaction

$$K^+ + \text{solid} \rightleftharpoons \beta/2\, Ca^{2+} + (1 - \beta)Na^+ + \text{solid} \quad (15)$$
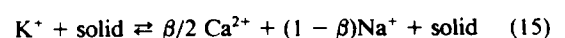
they arrived at a value of β = ⅓ for high temperature solutions corresponding to the reaction

$$K^+ + \text{solid} \rightleftarrows \tfrac{1}{6} Ca^{2+} + \tfrac{2}{3} Na^+ + \text{solid} \qquad (16)$$
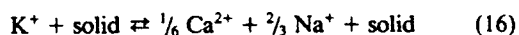
and of β = ⅘ for low temperature systems

$$K^+ + \tfrac{1}{3} Na^+ + \text{solid} \rightleftarrows \tfrac{2}{3} Ca^{2+} + \text{solid}. \qquad (17)$$

FOURNIER and TRUESDELL (1973) do not report any temperature dependences for these reactions, from their discussions it has to be concluded that they are taken to be independent of β and, therefore, are given by only one equation

$$\log K_{15} = \log (a_{Na^+}/a_{K^+}) + \beta \log (a_{Ca^{2+}}^{1/2}/a_{Na^+})$$

$$= (1647/T) - 2.24, \qquad (18)$$

a condition only valid if β is seen as a statistical weighing factor and not a stoichiometric coefficient.

The apparent success of the technique gave rise to a flurry of studies trying to provide its theoretical or experimental justification (SHIKAZONO, 1976; MICHARD and FOUILLAC, 1976; JANECKI et al., 1986). Quite early on, however, PAČES (1975) observed a systematic deviation for the Na-K-Ca geothermometer below 75°C and proposed a correction term involving P_{CO_2}. In 1977, FOUILLAC and MICHARD also pointed out problems arising in the application of this geothermometer to high CO_2 waters. In a valiant attempt to extend its validity range to lower temperatures, FOURNIER and POTTER (1979) proposed a Mg-correction. The general incompatibility of a common temperature dependence for two quite different reactions, one essentially based on the exchange of K for Na (Eqn. 16), the other of K and Na for Ca (Eqn. 17), was pointed out by ARNORSSON et al. (1983b) and BENJAMIN et al. in 1983. The latter derived two independent equations, valid below and above 100°C respectively and suggested that a range of alteration phases thermodynamically similar to feldspars, rather than feldspars themselves control relative cation contents. In another recent experimental study, POPE et al. (1987) found that the Na-K-Ca-geothermometer worked well for dilute chloride solutions but not in the case of $NaHCO_3$ solutions.

Based on these findings, it may be concluded that many of the problems associated with the application of the Na-K-Ca geothermometer arise from its sensitivity to variations in the CO_2-content of geothermal fluids especially at lower temperatures. Rather than forming the basis for a geothermometer, Ca-contents of lower temperature geothermal solutions, therefore, may to good advantage be used in the formulation of a valuable CO_2-geobarometer.

Well before the arrival of the Na-K-Ca-geothermometer, ELLIS (1970) had already pointed out the sensitivity of calcium contents to variations in the CO_2 content of thermal waters and had proposed a technique for the evaluation of deep CO_2-partial pressures by use of Na-Ca-contents. The procedure was based on the assumption of equilibrium of the waters with an assemblage containing feldspar, illite and calcite. Calcite is an ubiquitous mineral in geothermal systems (BROWNE, 1978) and geothermal discharges have been shown to be close to saturation with respect to calcite on many occasions (ARNORSSON et al., 1983b; WHITE, 1986).

The most important reaction leading to the formation of calcite in geothermal systems is the conversion of Ca-aluminium silicates to calcite by CO_2 of deep, probably magmatic origin, according to

$$Ca\text{-}Al\text{-silicate} + CO_2 + H_2O \rightleftarrows$$

$$CaCO_3 + 2(H\text{-}Al\text{-silicate}) \qquad (19)$$
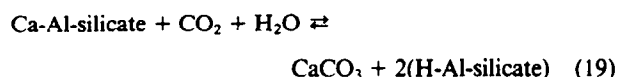
the "acid clays" thus formed promote further rock dissolution according to Eqn. (11). The minimum CO_2-fugacity required to allow reaction (19) to proceed is that corresponding to equilibrium of calcite with the full equilibrium mineral assemblage involving K-feldspar/K-mica according to

$$Ca\text{-}Al_2\text{-silicate} + K\text{-feldspar} + CO_2 \rightleftarrows$$

$$CaCO_3 + K\text{-mica}. \qquad (20)$$
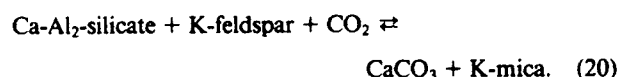
Its temperature dependence is adequately represented by log $f_{CO_2} = 0.0168t - 3.78$ where t is the temperature in °C (GIGGENBACH, 1984).

Initial CO_2-contents of deep geothermal fluids are likely to be externally controlled and to reflect largely variations in the relative proportions of CO_2-rich magmatic fluids and CO_2-poor meteoric water making up the rising fluid (Fig. 1). For any such rising fluid, there exists, a range of conditions where f_{CO_2}-values are likely to be below those of reaction (20) and therefore too low to induce calcite formation. Full equilibrium f_{CO_2}-values, however, drop rapidly with decreasing temperature (Eqn. 20) and any rising geothermal fluid with a given CO_2 content can be expected to become reactive (GIGGENBACH, 1984) with respect to CO_2-induced hydrogen metasomatism and deposition of calcite at some stage.

Rather than starting from the high Al_H-end of the silica saturation lines in Fig. 6, the reaction path describing the interaction of rising CO_2-containing geothermal fluids then is likely to hover in the vicinity of the full equilibrium point, deviating significantly to higher Al_H-values only when relative rates of cooling of the fluids become much faster than those of re-equilibration with the rock. The chemical environment prevailing during the conversion of CO_2 to calcite, over large parts of a geothermal system, therefore, is likely to correspond closely to that governed by the full equilibrium buffer and the reaction linking CO_2-fugacity and water chemistry may be written in terms of endmembers as

$$3K\text{-feldspar} + CO_2 + Ca^{2+} \rightleftarrows$$

$$\text{muscovite} + \text{calcite} + 6 \text{ silica} + 2K^+ \qquad (21)$$
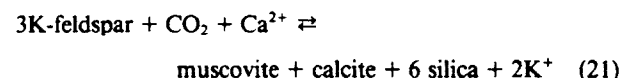
its equilibrium constant corresponds to

$$K_{21} = (a_{K^+}^2/a_{Ca^{2+}} \cdot f_{CO_2})(a_{musc} \cdot a_{calcite} a_{silica}^6/a_{microcline}^3). \qquad (22)$$

Again the assumption $\gamma_1^2 = \gamma_2$ is made, silica activities are assumed to be those of chalcedony solubility and ($a_{muscovite}a_{calcite}/a_{microcline}^3$) is set to unity. Under these circumstances the values of $L_{21} = \log K_{21}$ as calculated by data given by BOWERS et al. (1984) are with -1.66 ± 0.15 from 50° to 300° almost temperature independent. Together with the conversion factor from activities to mg/kg (Eqn. 1), the relationship linking analytical K- and Ca-contents to f_{CO_2} is for practical purposes adequately given by

$$L_{kc} = \log (c_{K^+}^2/c_{Ca^{2+}}) = \log f_{CO_2} + 3.0. \qquad (23)$$

Application of Eqn. (23) again is, of course, limited to systems for which close approach of equilibrium with all the mineral phases involved in reaction (21) can be assumed. In the absence of calcite the correlation between L_{kc} and CO_2 does not apply.

Notwithstanding the temperature independence of L_{kc}, CO_2-fugacities in geothermal systems are strongly dependent on temperature. In order to be able to correlate the CO_2-fugacities obtained by use of Eqn. (23) to their likely equilibration reference temperature, a geothermometer equilibrating with similar speed and under similar conditions to that of the K-Ca-geobarometer is required. The nearest such system is likely to be that involving K and Mg as described above. The overall geobarometer then again is based on three solution components and, therefore, would be suitable for evaluation by use of a triangular diagram. Because of the intricate correlations among f_{CO_2} and the CO_2-contents of coexisting liquid and vapor phases, a more open presentation as shown in Fig. 10 is preferred.

Analytical values of L_{kc} are plotted against L_{km}. Again a line representing full fluid-rock equilibrium (Eqn. 20) is shown together with stability boundaries for Ca-Al-silicates (GIGGENBACH, 1984). Data points below the full equilibrium line correspond to the compositions of comparatively immature fluids with higher than full equilibrium CO_2 fugacities and, therefore, being reactive with respect to hydrogen metasomatism. Values above this line (ZU, CP, TO) are likely to reflect comparatively low proportions of deep CO_2-rich vapors contributing to the geothermal fluid at depth. In these systems the CO_2-contents of the fluid tapped by the drillhole are too

low to lead to CO_2 attack on Ca-aluminium silicates and the formation of calcite. The values of f_{CO_2} obtained then provide only a qualitative indication. The relative positions of most of the well and associated spring discharges, straddling the full equilibrium line, however, clearly indicate attainment of CO_2-fugacities conducive to the formation of calcite at some stage during the rise of these waters to the surface.

The CO_2-fugacities derived by use of the K- and Ca-contents of some of the well discharges (Eqn. 23) may be compared to those obtained on the basis of measured total discharge gas contents. Assuming the gases to have been dissolved in a single liquid phase, the compositions of steam discharged from Wairakei and Broadlands wells (GIGGENBACH, 1980) correspond to CO_2-fugacities of between 0.2 to 1.1 b and 7.0 to 17 b, respectively. The upper limits, likely to be most representative of the undisturbed state of these systems, agree exactly with those obtained on the basis of K- and Ca-contents (Fig. 10).

The data points for the acid waters fall all well below the full equilibrium line, a behaviour not too surprising taking into account the certain absence of calcite and feldspars in the mineral suites coexisting with these waters. Comparison with the lines representing the dissolution of varying amounts of average crustal rocks (Table 1) clearly shows again that their composition is controlled by rock dissolution rather than equilibration. For such waters, already identified as immature by use of Fig. 9, evaluation of equilibration f_{CO_2} by use of their K-Ca-contents is not possible.

Of the eight soda spring waters, almost all plot close to the rock dissolution lines. Again taking into account the immature nature of these waters as indicated by Fig. 9 this is quite expected. The two soda spring waters showing some
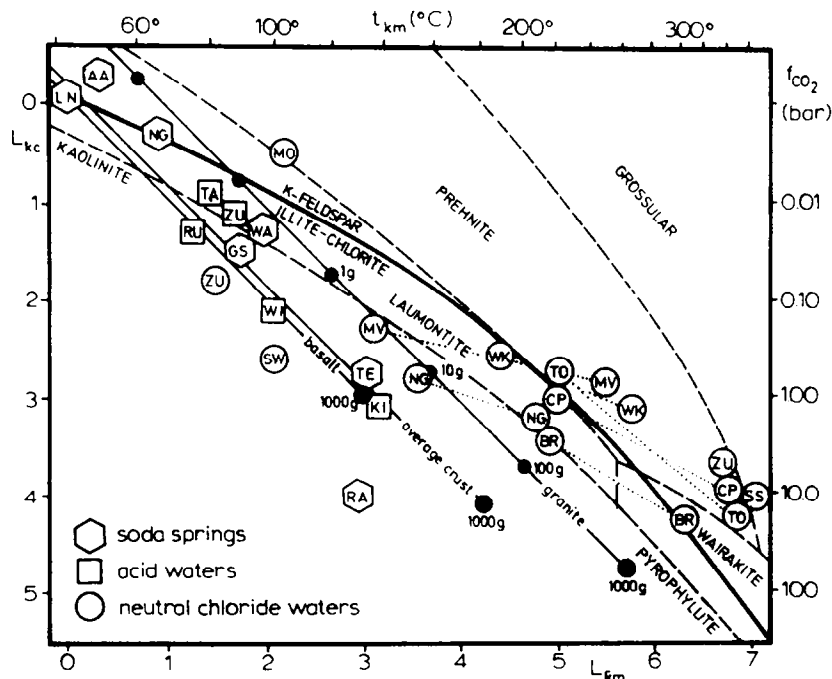

FIG. 10. Evaluation of CO_2-fugacities in geothermal systems by use of K, Mg and Ca contents of their discharge waters. For symbols see Table 1 and Fig. 2. The stability fields of some Ca-Al-silicates are shown as a function of f_{CO_2} and temperature together with lines representing solutions of typical crustal rocks.

apparent approach to fluid/rock-equilibrium, those from Te Aroha (TE) and Radkersburg (RA) (Fig. 9), give equilibration temperatures of around 130° at CO_2-fugacities of 0.9 and 10 b, respectively. Both are associated with active deposition of calcite at the surface thus confirming calcite supersaturation, at least under surface discharge conditions. Deposition of calcite at shallow levels or even during sampling may then be responsible for the very low Ca-content of the Radkersburg sample and the correspondingly very high apparent CO_2-fugacity. The CO_2 pressure indicated for the Te Aroha water of around 1 bar is that expected for such lower temperature, calcite depositing springs.

From the above findings it can be concluded that evaluation of f_{CO_2} by use of K-Ca contents of discharge waters is only reliable for data points close to the full equilibrium line. For data points deviating significantly, the full equilibrium line may be taken to separate waters from two distinct alteration environments: those plotting below in Fig. 10 are likely to come from an alteration system dominated by acid fluids, those plotting above from a rock dominated, CO_2-deficient environment.

PRACTICAL APPLICATIONS

The wide range of chemical geothermometers hitherto proposed and to varying degrees presently in use may be subdivided into several categories, depending on the number of components involved in their formulation. The most simple ones are those based on uni-variant reactions such as the silica geothermometer and a number of gas geothermometers as proposed by ARNORSSON et al. (1983a,b) and discussed by ARNORSSON and SVAVARSSON (1985). Their major disadvantage is their high sensitivity to secondary processes such as dilution, and in the case of gas geothermometers, to vapor loss or condensation and errors in the estimates of vapor-liquid ratios.

At the other end of the spectrum are "global" techniques involving a large number of constituents and based on the inherent assumption that all these constituents have been in equilibrium simultaneously at some stage and that their compositions are still representative of the conditions in this deeper equilibration zone. Examples are gas geothermometers proposed by GIGGENBACH (1980) on the basis of reactions involving the formation of CH_4 and NH_3, or those based on the reconstruction of the deep equilibrium fluid as proposed, e.g., by MICHARD and ROEKENS (1983) and REED and SPYCHER (1984).

Application of these techniques is valid in the case of deep well discharges likely to be representative of the deep equilibrium environment, but questionable in the case of natural surface discharges. For these fluids, subject to secondary processes such as partial re-equilibration to lower temperatures, dilution or steam loss, the results become inconclusive. Major disadvantages of these multicomponent techniques then are their dependence on virtually complete and representative analyses of thermal discharges and on the availability of reliable thermodynamic information for a large number of mineral and fluid phase species, their limited ability to allow any further ready interpretation or intercomparison among a large number of samples and their general unwieldiness. A useful aspect of these global techniques is their ability to reveal attainment of equilibrium among a large number of fluid and mineral components. Under these circumstances, however, any geoindicator based on a suitable subsystem,

involving much fewer components, would have given the same answer.

Most of the drawbacks of single species and global techniques are overcome by the use of isomolar concentration ratios in the case of gases (GIGGENBACH, 1987) or isocoulombic concentration quotients, as discussed above, in the case of ionic solutes. These approaches are in accordance with the general rule that comparison of analytical and theoretical information in geochemical systems should be carried out as much as possible on the basis of actually measured variables and variable by variable (GIGGENBACH, 1987). The two diagrams represented by Figs. 9 and 10, based on readily available analytical information, fulfil this condition; the overall treatment essentially preserves the identity of each variable and allows secondary processes affecting each variable to be assessed individually.

The above findings also show that one of the most important additional requirements in the formulation of a geoindicator is the strict delineation of its limits of applicability. In the graphical evaluation of water-rock equilibration by use of Fig. 9, two areas marked partially equilibrated waters and immature waters were distinguished. They are defined by the full equilibrium line and another apparently quite arbitrary curve separating the area where the Na-K-Mg-geothermometer may be applied with confidence from one representing immature waters likely to reflect the effects of rock dissolution rather than rock equilibration. In order to facilitate numerical evaluation, a "maturity index" measuring the degree of attainment of water-rock equilibrium would be useful. Such an index may be obtained by first combining the Na-K- and K-Mg-geothermometers as represented by the equations

$$t_{kn} = 1390/(1.75 - L_{kn}) - 273.2 \qquad (24)$$

$$t_{km} = 4410/(14.0 - L_{km}) - 273.2 \qquad (25)$$

to form a temperature independent equation for the full equilibrium curve according to

$$L_{kn} = 0.315 L_{km} + 2.66 = s L_{km} + MI \qquad (26)$$

or

$$c_{Na} = 457 c_K^{0.37} c_{Mg}^{0.315} = mi c_K^{(1-2s)} c_{Mg}^{s}. \qquad (27)$$

The coefficient $s = 0.315$ represents the ratio of van't Hoff slopes for the two geothermometers, the value of $mi = 457$ the concentration of sodium required for given values of $c_K^{0.37} c_{Mg}^{0.315}$ to obtain full equilibrium. As discussed in detail above (Fig. 8), the major cause of non-attainment of water-rock equilibrium in geothermal solutions approaching full equilibrium is the slowness of the process supplying the comparatively large equilibrium contents of Na especially in lower temperature solutions. Lack of equilibrium, therefore, is likely to be reflected in Na-contents of the waters being too low. The apparently quite arbitrary line in Fig. 9 separating immature from partially equilibrated waters actually corresponds to a value of MI, the "maturity index", of 2.0 according to

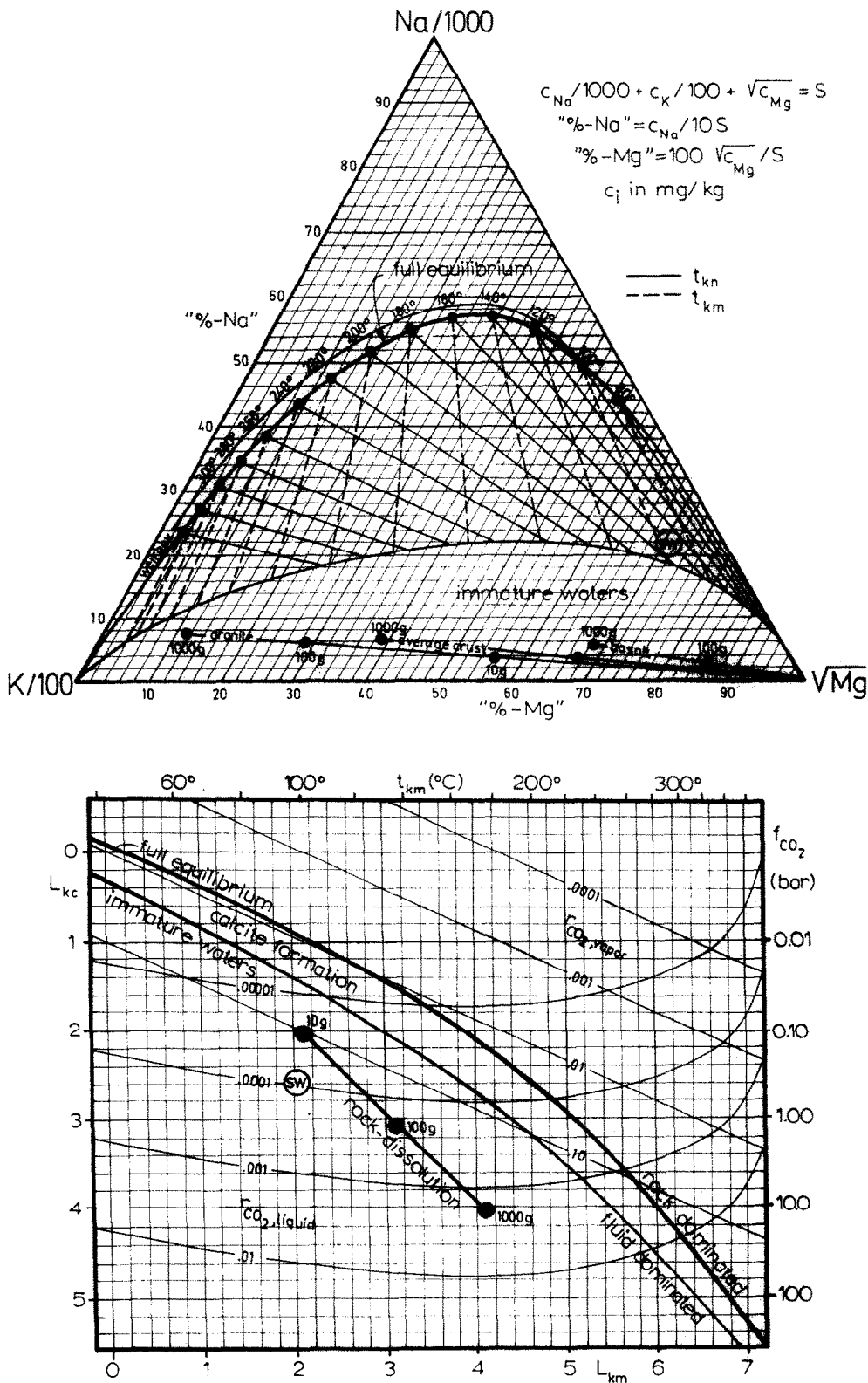$$MI = 0.315 L_{km} - L_{kn} = 2.0 \qquad (28)$$

FIG. 11. Blank diagrams for the evaluation of Na-K and K-Mg equilibration temperatures (A) and of CO_2-fugacities (B) by use of Na, K, Mg and Ca contents of thermal waters. The CO_2-contents of liquid and vapor phases as a function of f_{CO_2} and temperature are only valid for low salinity systems. The rock dissolution line of Fig. 11b refers to solutions of 10, 100, 1000 g of an average crustal rock in 1 kg of water.

or

$$c_{Na} = 100 c_K^{0.37} c_{Mg}^{0.315}. \tag{29}$$

The curve thus defined, however, should only be taken as a rough guideline as the reliability of the Na-K-Mg-geothermometer is likely to decrease gradually with MI, the reliability of t_{kn} decreasing more rapidly than that of t_{km}. The main value of the MI = 2.0 curve lies in its use of distinguishing waters suitable for the application of the K-Mg-Ca-geobarometer or not.

Equations (24), (25) and (28) allow a purely numerical evaluation of the Na-K-Mg-geoindicator. The graphical technique of Fig. 9, however, has the advantage of allowing simultaneous evaluation of a large number of samples, a preliminary visual statistical assessment and the delineation of trends and groupings. In order to facilitate application of the graphical technique a blank version of Fig. 9 is given in Fig. 11a. It may be photocopied or reproduced by use of the data given in Table 2. Relative Na, K, Mg-contents required in plotting the curve for MI = 2.0 by computer may be obtained from Eqn. (29) by setting c_K to unity or by dividing the amounts of Na given in Table 2 by 4.57.

Figure 11a also contains a curve marked weirbox, it describes the position of waters subject to maximum steam loss through flashing from their full equilibrium temperature to 100°C. Again lines for rock dissolution are given, they represent the composition of waters resulting from the dissolution of varying amounts of crustal rocks (Table 1) in 1 kg of water.

For waters plotting below the full equilibrium line, K-Mg-temperatures are lower than K-Na-temperatures. Because of the faster rate of equilibration in the system K-Mg, values of t_{km} are likely to reflect conditions at shallower levels, with t_{kn} those at considerable depth. A number of additional processes such as admixture of immature waters with their generally high Mg-contents will also lead to deviations from the full equilibrium curve and to different K-Na- and K-Mg-tem-

peratures. Simple dilution by non-mineralised waters also causes minor shifts in the position of data points towards the Mg-corner. In the case of boiling chloride springs, even if unaffected by admixture of immature waters, K-Na-temperatures are likely to reflect minimum values, deep temperatures being often considerably higher as shown by the position of data points for well and associated spring samples in Fig. 9.

Close attainment of water-rock equilibrium even at lower temperatures, e.g. in essentially stagnant reservoirs of formation waters, is indicated by the water discharged at Morere (MO). Seawater has a maturity index of 2.09 well below that expected for full equilibrium of 2.66. Both t_{kn} of 162°C and t_{km} of 97°C possibly reflect the high temperatures of its interaction with basaltic material along mid-ocean ridges.

As pointed out above, before applying the K-Mg-Ca-geobarometer the suitability of a water should be checked by use of Fig. 11a or by determining its maturity index which should be above 2.0. Again a blank diagram is presented in Fig. 11b. The curves relating CO_2-fugacities and the CO_2-contents of coexisting vapor and liquid phases were drawn by use of data given in Table 2 assuming ideal gas behaviour and may, therefore, be applied only to low salinity systems (<0.1 m) at pressures < 100 bar. The relationships used are

$$f_{CO_2} = r_{CO_2,v} f_{H_2O}$$

$$= r_{CO_2,l} B_{CO_2} f_{H_2O} \tag{30}$$

where r_{CO_2} are the mole-ratios n_{CO_2}/n_{H_2O} in the vapor and liquid phase respectively, f_{H_2O} the vapor pressure of water and B_{CO_2} the distribution coefficient $r_{CO_2,v}/r_{CO_2,l}$ of CO_2 at a given temperature. The temperature dependences of f_{H_2O} and B_{CO_2} (GIGGENBACH, 1980) are given, with adequate precision, by

$$\log f_{H_2O} = 5.51 - 2048/(t + 273.2) \tag{31}$$

$$\log B_{CO_2} = 4.7593 - 0.01092t \tag{32}$$

with t in °C.

The CO_2-content of the fluids in wt% may be obtained from the values of r_{CO_2} by use of

$$\%CO_2 \text{ b.w.} = 244 r_{CO_2}/(1 + 2.44 r_{CO_2}). \tag{33}$$

The full equilibrium line is given by Eqn. (20) and may be expressed in terms of L_{km} according to

$$L_{kc} = \log (c_K^2/c_{Ca})$$

$$= \log f_{CO_2} + 3.0$$

$$= 0.0168t - 0.78$$

$$= 74.09/(14.0 - L_{km}) - 5.37. \tag{34}$$

Again the ranges of water compositions resulting from the dissolution of 10, 100 and 1000 g of an average crustal rock (Table 1) in 1 kg of water are shown. By applying Fig. 11b only to waters with MI > 2.0, those reflecting rock dissolution should have already been eliminated. In spite of its low maturity index of 2.06, just within the applicability range of 2.0 to 2.66, the data point for seawater is also given in Fig. 11b. Its position again is far from the full equilibrium line but quite close to the basalt dissolution line (Fig. 10) suggesting that seawater represents a solute system far from any equilibrium involving minerals likely to control fluid chemistry in geothermal systems.

TABLE II

Data useful in the construction of Figs 11A and 11B, c_j in mg/kg, f_j in bar. Number of eqn in brackets.

t°C	c_{Na} (12)	c_K	c_{Mg} (13)	f_{H_2O}	B_{CO_2} (32)	f_{CO_2} (20)
20°	97 900	100	109880	0.02	34 750	.0004
40°	48 759	100	12035.	0.07	23 010	.0008
60°	26 404	100	1719.0	0.20	12 710	.0017
80°	15 327	100	306.10	0.47	7 690	.0037
100°	9 431	100	65.600	1.01	4 650	.0079
120°	6 097	100	16.430	1.98	2 810	.0172
140°	4 111	100	4.7080	3.61	1 700	.0373
160°	2 875	100	1.5140	6.18	1 030	.0809
180°	2 075	100	0.5380	10.02	622	.1754
200°	1 540	100	0.2090	15.54	376	.3800
220°	1 170	100	0.0874	23.18	227	.8240
240°	909	100	0.0392	33.44	138	1.787
260°	719	100	0.0187	46.88	83	3.870
280°	579	100	0.0094	64.12	50	8.395
300°	473	100	0.0049	85.81	30	18.20
320°	392	100	0.0027	112.70	18	39.45
340°	329	100	0.0016	145.90	11	85.50

Figure 10 also contains stability ranges of Ca-aluminium silicates as a function of f_{CO_2} and temperature as derived earlier (GIGGENBACH, 1984). Minerals commonly observed in geothermal alteration assemblages (BROWNE, 1978), but with highly variable and frequently unknown compositions, such as smectites and epidotes, have been omitted. Their potential stability ranges overlap with those of their thermodynamic proxies laumontite and wairakite. With increasing f_{CO_2} the latter are converted to kaolinite or pyrophyllite. The corresponding boundaries describe maximum CO_2 fugacities for the formation of calcite from Ca-aluminium silicates according to reaction (19) and delineate, together with the full equilibrium curve (Eqn. 20), the range of calcite formation in rising geothermal fluids and, therefore, the range of applicability of the K-Ca-geobarometer. A simplified eqn describing this upper f_{CO_2} limit, valid from 80° to 320°C. is

$$\log f_{CO_2} = 0.0185t - 3.48. \tag{35}$$

Data points outside this range are likely to represent waters from highly immature alteration systems dominated by acid fluids or from rock dominated alteration systems with low reactivities of CO_2, as indicated. The effects of a series of secondary processes such as conductive cooling, dilution and boiling on f_{CO_2} have been discussed in detail earlier (GIGGENBACH, 1984).

The above techniques were derived for rising hydrothermal solutions where interaction with the rock can be assumed to consist largely of initial rock dissolution in waters formed through absorption of magmatic vapors followed by more gentle H-metasomatism associated with the conversion of CO_2 to calcite and of "acid" clays to "neutral" aluminium silicates. The other major alteration process is K-metasomatism in major upflow zones in response to conductive or isenthalpic (boiling) cooling (GIGGENBACH, 1984). For other systems the above techniques may, in modified form, still be applicable. In the case of seawater driven alteration systems (SEYFRIED and BISCHOFF, 1981) the starting fluid is obviously seawater; in the case of interaction of fluids derived through leaching of evaporitic material, initial water compositions may be characterised by the predominance of sodium with the full-equilibrium curve of Fig. 9 being approached from the Na-corner.

Editorial handling: E. J. Reardon

REFERENCES

ARNORSSON S. and SVAVARSSON H. (1985) Application of chemical geothermometry to geothermal exploration and development. *Geoth. Resources Council, Trans.* **9**, 293–298.

ARNORSSON S., GUNNLAUGSSON E. and SVAVARSSON H. (1983a) The chemistry of geothermal waters in Iceland. II. Mineral equilibria and independent variables controlling water compositions. *Geochim. Cosmochim. Acta* **42**, 523–536.

ARNORSSON S., GUNNLAUGSSON E. and SVAVARSSON H. (1983b) The chemistry of geothermal waters in Iceland. III. Chemical geothermometry in geothermal investigations. *Geochim. Cosmochim. Acta* **42**, 567–577.

BENJAMIN T., CHARLES R. and VIDALE R. (1983) Thermodynamic parameters and experimental data for the Na-K-Ca-geothermometer. *J. Volcanol. Geoth. Res.* **15**, 167–186.

BORISOV M. V., RYZHENKO B. N. and KRAYNOV S. R. (1985) Influence of the acid-base properties of rocks on the composition of equilibrated aqueous solutions. *Geochemistry Intl.*, pp. 87–94.

BOWERS T. S., JACKSON K. I. and HELGESON H. C. (1984) *Equilibrium Activity Diagrams.* Springer-Verlag.

BRIMHALL G. H. and GHIORSO M. S. (1983) Origin and ore-forming consequences of the advanced argillic alteration process in hypogene environments by magmatic gas contamination of meteoric fluids. *Econ. Geol.* **78**, 73–90.

BROWNE P. R. L. (1978) Hydrothermal alteration in active geothermal fields. *Ann. Rev. Earth Plant. Sci.* **6**, 229–250.

BURNHAM C. W. (1979) Magmas and hydrothermal fluids. In *Geochemistry of Hydrothermal Ore Deposits* (ed. H. L. BARNES), pp. 71–136. J. Wiley & Sons.

CAPUANO R. M. and COLE D. R. (1982) Fluid-mineral equilibria in a hydrothermal system, Roosevelt Hot Springs, Utah. *Geochim. Cosmochim. Acta* **46**, 1353–1364.

CATHLES L. M. (1977) An analysis of the cooling of intrusives by groundwater convection which includes boiling. *Econ. Geol.* **72**, 804–826.

CHOU L. and WOLLAST R. (1984) Study of the weathering of albite at room temperature and pressure with a fluidized bed reactor. *Geochim. Cosmochim. Acta* **48**, 2205–2217.

ELLIS A. J. (1970) Quantitative interpretation of chemical characteristics of hydrothermal systems. *Geothermics* **2**, 516–528.

ELLIS A. J. (1971) Magnesium ion concentrations in the presence of magnesium chlorite, calcite, carbon dioxide, quartz. *Amer. J. Sci.* **271**, 481–489.

ELLIS A. J. and MAHON W. A. J. (1964) Natural hydrothermal systems and experimental hot water/rock interactions. *Geochim. Cosmochim. Acta* **28**, 1323–1357.

ELLIS A. J. and MAHON W. A. J. (1967) Natural hydrothermal systems and experimental hot water/rock interactions (Part II). *Geochim. Cosmochim. Acta* **31**, 519–538.

ELLIS A. J. and MAHON W. A. J. (1977) *Chemistry and Geothermal Systems.* Academic Press, 392p.

ELLIS A. J. and WILSON S. H. (1960) The geochemistry of alkali metal ions in the Wairakei hydrothermal system. *N. Z. J. Geol. Geophys.* **3**, 593–617.

EUGSTER H. P. (1985) Granites and hydrothermal ore deposits: A geochemical framework. *Mineral Mag.* **49**, 7–23.

FOUILLAC C. and MICHARD G. (1977) Sodium, potassium, calcium relationships in hot springs of Massif Central. *Proc. 2nd Intl. Symp. on Water-Rock Interaction, Strasbourg* **3**, 109–116.

FOURNIER R. O. (1979) A revised equation for the Na/K geothermometer. *Geoth. Resources Council, Trans.* **3**, 221–224.

FOURNIER R. O. and POTTER R. W. (1979) Magnesium correction to the Na-K-Ca chemical geothermometer. *Geochim. Cosmochim. Acta* **43**, 1543–1550.

FOURNIER R. O. and TRUESDELL A. H. (1973) An empirical Na-K-Ca geothermometer for natural waters. *Geochim. Cosmochim. Acta* **37**, 1255–1275.

GIGGENBACH W. F. (1975a) Variations in the carbon, sulfur and chlorine contents of volcanic gas discharges from White Island, New Zealand. *Bull. Volcanol.* **39**, 15–27.

GIGGENBACH W. F. (1975b) The chemistry of Crater Lake, Mt. Ruapehu (New Zealand) during and after the 1971 active period. *New Zealand J. Sci.* **17**, 33–45.

GIGGENBACH W. F. (1977) The isotopic composition of sulphur in sedimentary rocks bordering the Taupo Volcani Zone. In *Geochemistry 1977; NZ DSIR Bull. 218*, pp. 57–64.

GIGGENBACH W. F. (1980) Geothermal gas equilibria. *Geochim. Cosmochim. Acta* **44**, 2021–2032.

GIGGENBACH W. F. (1981) Geothermal mineral equilibria. *Geochim. Cosmochim. Acta* **45**, 393–410.

GIGGENBACH W. F. (1984) Mass transfer in hydrothermal alteration systems. *Geochim. Cosmochim. Acta* **48**, 2693–2711.

GIGGENBACH W. F. (1985) Construction of thermodynamic stability diagrams involving dioctahedral potassium clay minerals. *Chem. Geol.* **49**, 231–242.

GIGGENBACH W. F. (1987) Redox processes governing the chemistry of fumarolic gas discharges from White Island, New Zealand. *Appl. Geochem.* **2**, 143–161.

GIGGENBACH W. F. (1988) Water and gas chemistry of Lake Nyos, Cameroon, and its bearing on the eruptive process. *J. Volcanol. Geoth. Res.* (in press).

GIGGENBACH W. F. and GLASBY G. P. (1977) The influence of thermal activity on the trace metal distribution in marine sediments around White Island, New Zealand. *NZ DSIR Bull.* **218**, 121–126.

GIGGENBACH W. F. and LE GUERN F. (1976) The chemistry of magmatic gases from Erta'Ale, Ethiopia. *Geochim. Cosmochim. Acta* **40**, 25–30.

GIGGENBACH W. F., GONFIANTINI R., JANGI B. L. and TRUESDELL A. H. (1983) Isotopic and chemical composition of Parbati Valley geothermal discharges, NW-Himalaya, India. *Geothermics* **12**, 199–222.

GOGUEL R. L. (1983) The rare alkalies in hydrothermal alteration at Wairakei and Broadlands geothermal fields, NZ. *Geochim. Cosmochim. Acta* **47**, 429–437.

HEMLEY J. J. (1967) Aqueous Na/K ratios in the system $K_2O-Na_2O-Al_2O_3-SiO_2-H_2O$. *Program, 1967 Ann. Meeting, Geol. Soc. Amer. New Orleans*, pp. 94–95.

HEMLEY J. J. and JONES W. R. (1964) Chemical aspects of hydrothermal alteration with emphasis on hydrogen metasomatism. *Econ. Geol.* **59**, 538–369.

HENLEY R. W. and MCNABB A. (1978) Magmatic vapor plumes and groundwater interaction in porphyry copper emplacement. *Econ. Geol.* **73**, 1–20.

HENLEY R. W., TRUESDELL A. H., BARTON P. B. and WHITNEY J. A. (1984) Fluid-mineral equilibria in hydrothermal systems. *Rev. in Econ. Geol.* **1**, 267.

HOLDREN G. R. and SPEYER P. M. (1985) pH dependent changes in the rates and stoichiometry of dissolution of an alkali feldspar at room temperature. *Amer. J. Sci.* **285**, 994–1026.

HOLLAND H. D. (1972) Granites, solutions and base metal deposits. *Econ. Geol.* **67**, 281–301.

JANECKI D. R., CHARLES R. W., BAYHURST G. K. and BENJAMIN T. M. (1986) The physicochemical basis of the Na-K-Ca geothermometer. *Los Alamos Report LA-10806 MS*, 10p.

KRUPP R. E. and SEWARD T. M. (1987) The Rotokawa geothermal system, New Zealand: An active epithermal gold-depositing environment. *Econ. Geol.* **82**, 1109–1129.

LINDSAY T. W. (1980) Estimation of concentration quotients for ionic equilibria in high temperature water: The model substance approach. *Proc. Intl. Water Conf., Pittsburgh*, pp. 284–294.

LOWELL J. D. and GUILBERT J. M. (1970) Lateral and vertical alteration-mineralisation zoning in porphyry ore deposits. *Econ. Geol.* **65**, 373–408.

MICHARD G. and FOUILLAC C. (1976) Remarques sur le thermomètre Na-K-Ca. *J. Volcanol. Geoth. Res.* **1**, 297–307.

MICHARD G. and ROEKENS E. (1983) Modelling of the chemical composition of alkaline hot waters. *Geothermics* **12**, 161–169.

ORVILLE P. M. (1963) Alkali ion exchange between vapor and feldspar phases. *Amer. J. Sci.* **261**, 201–237.

PAČES T. (1975) A systematic deviation from Na-K-Ca geothermometer below 75°C and above 10^{-4} atm P_{CO_2}. *Geochim. Cosmochim. Acta* **39**, 541–544.

PETIT J. C., GIANANTONIO D. M., DRAN J. C., SCHOTT J. and BERNER R. A. (1987) Mechanism of diopside dissolution from hydrogen depth profiling. *Nature* **325**, 705–707.

POPE L. A., HAJASH A. and POPP R. K. (1987) An experimental investigation of quartz, Na-K, Na-K-Ca geothermometers and the effects of fluid composition. *J. Volcanol. Geoth. Res.* **31**, 151–161.

REED M. and SPYCHER N. (1984) Calculation of pH and mineral equilibria in hydrothermal waters with application to geother-mometry and studies of boiling and dilution. *Geochim. Cosmochim. Acta* **48**, 1479–1492.

ROSE W. I., CHUAN R. L., GIGGENBACH W. F., KYLE P. R. and SYMONDS R. B. (1986) Rates of sulfur dioxide emissions from White Island volcano, New Zealand, and an estimate of the total flux of major gaseous species. *Bull. Volcanol.* **48**, 181–188.

RUAYA J. R. and SEWARD T. M. (1987) The ion-pair constant and other thermodynamic properties of HCl up to 350°C. *Geochim. Cosmochim. Acta* **51**, 121–130.

SASS B. E., ROSENBERG P. E. and KITTRICK J. A. (1987) The stability of illite/smectite during diagenesis: An experimental study. *Geochim. Cosmochim. Acta* **51**, 2103–2115.

SAVAGE D. (1986) Granite-water interactions at 100°, 50 MPa: An experimental study. *Chem. Geol.* **54**, 81–95.

SAVAGE D., CAVE M. R., MILDOWSKI A. E. and GEORGE I. (1987) Hydrothermal alteration of granite by meteoric fluid: An example from the Carnmellis Granite, United Kingdom. *Contrib. Mineral. Petrol.* **96**, 391–405.

SCHRAMKE J. A., KERRICK D. M. and LASAGA A. C. (1987) The reaction muscovite+quartz $\rightleftarrows$ andalusite+K-feldspar+water. Part I. Growth kinetics and mechanism. *Amer. J. Sci.* **287**, 517–559.

SCHOEN R., WHITE D. E. and HEMLEY J. J. (1974) Argillization by descending acid at Steamboat Springs, Nevada. *Clays Clay Mineral.* **22**, 1–22.

SEYFRIED W. E. and BISCHOFF J. L. (1981) Experimental seawater-basalt interaction at 300°C, 500 bars; chemical change, secondary mineral formation and implications for the transport of heavy metals. *Geochim. Cosmochim. Acta* **45**, 135–147.

SHIKAZONO N. (1976) Thermodynamic interpretation of Na-K-Ca geothermometer in the natural water system. *Geochem. J.* **10**, 47–50.

SHIKAZONO N. (1978) Possible cation buffering in chloride-rich geothermal waters. *Chem. Geol.* **23**, 239–254.

SILLITOE R. H. (1973) The tops and bottoms of porphyry copper deposits. *Econ. Geol.* **68**, 799–815.

STOFFREGEN R. E. (1985) Genesis of acid-sulfate alteration and Au-Cu-Ag mineralisation at Summitville, Colorado. Ph.D. thesis. Univ. of California, Berkeley, 205p.

TAYLOR S. R. (1964) Abundance of chemical elements in the continental crust, a new table. *Geochim. Cosmochim. Acta* **28**, 1273–1285.

THOMPSON J. F. H., LESSMAN J. and THOMPSON A. J. B. (1986) The Temora gold-silver deposit: A newly recognised style of high sulfur mineralisation in the Lower Paleozoic of Australia. *Econ. Geol.* **81**, 732–738.

TRUESDELL A. H. (1975) Geochemical techniques in exploration. *Proc. 2nd UN Symp. on the Development and Use of Geothermal Resources* **1**, 53–86.

WALSHE J. L. (1986) A six-component chlorite solid solution model and the conditions of chlorite formation in hydrothermal and geothermal systems. *Econ. Geol.* **81**, 681–703.

WHITE D. E. (1957) Magmatic, connate, and metamorphic waters. *Geol. Soc. Amer. Bull.* **69**, 1659–1682.

WHITE A. (1986) Chemical and Isotopic characteristics of fluids within the Baca geothermal reservoir, Valles Caldera, New Mexico. *J. Geophys. Res.* **91**, 1855–1866.

WHITE D. E. (1965) Saline waters of sedimentary rocks. In *Fluids in Subsurface Environments*. Symp. Amer. Assoc. of Petroleum Geologists, pp. 342–366.